NASA TECHNICAL NOTE

NASA TN D-2169

C. 1

LOAN COPY: RE
AFWL (WLL
KIRTLAND AFB,

TECH LIBRARY KAFB, NM
0154404

NASA TN D-2169

EFFECT OF INTERCHANGING PROPELLANTS ON ROCKET COMBUSTOR PERFORMANCE WITH COAXIAL INJECTION

by Martin Hersch

Lewis Research Center
Cleveland, Ohio

NATIONAL AERONAUTICS AND SPACE ADMINISTRATION • WASHINGTON, D. C. • FEBRUARY 1964

TECH LIBRARY KAFB, NM
0154404

EFFECT OF INTERCHANGING PROPELLANTS ON ROCKET COMBUSTOR PERFORMANCE WITH COAXIAL INJECTION

By Martin Hersch

Lewis Research Center
Cleveland, Ohio

NATIONAL AERONAUTICS AND SPACE ADMINISTRATION

For sale by the Office of Technical Services, Department of Commerce,
Washington, D.C. 20230 -- Price $0.75

EFFECT OF INTERCHANGING PROPELLANTS ON ROCKET COMBUSTOR PERFORMANCE WITH COAXIAL INJECTION

SUMMARY

The effect of reversing propellants in coaxial injection on combustor performance was determined with a nominal-200-pound-thrust rocket combustor burning gaseous hydrogen with liquid oxygen. Reversing propellants refers to the change from oxidant in the tube to fuel in the tube.

The effect of this change was determined by measuring characteristic-velocity efficiency for a combustor having two interchangeable injectors. The injectors were designed so that the propellants could be reversed without changing their respective injection flow areas. The performance was evaluated for three chamber lengths over a range of oxidant-fuel weight ratios from about 1.5 to 10 and for various total propellant flow rates.

Higher performance was obtained when the liquid oxygen was injected from the annulus. Comparison of the data with those from analytical studies indicated that the performance could be reasonably correlated with a turbulent-mixing model, but a vaporization-limited model could not reasonably correlate the data for the tubular oxygen injection system.

It was also observed that the combustion noise level was lower with annularly injected liquid oxygen. Also, with annular oxygen injection, the injector face was less subject to high heat-transfer rates.

INTRODUCTION

Experimental studies (refs. 1 and 2) have demonstrated that coaxial flow injection gives high performance in rocket combustors. In this type of injection, one propellant is injected from the tube and the other propellant from the surrounding annulus.

When hydrogen and oxygen are used, it is common practice to inject the oxygen from the tube. As indicated in reference 1, however, it is thought that for better combustor performance the more volatile propellant should be injected from the tube. The reason for this is twofold. First, the more volatile propellant, in this case, the nearly gasified liquid hydrogen, when injected from a tube, will expand into the hollow cylinder of liquid that surrounds it. It will,

therefore, mix with this liquid and help to atomize it. Second, as pointed out in reference 1, the drop size of the less volatile propellant might be smaller when it is injected from a thin annulus rather than from a tube of the same area. It is assumed that the diameter of the tube and the thickness of the annulus are important in determining drop size, which in turn affects combustor performance (ref. 3).

The purpose of this study, therefore, was to determine the effect of reversing propellants on rocket combustor performance. The tests were conducted on a gaseous-hydrogen - liquid-oxygen combustor having two interchangeable injectors permitting propellant reversal; that is, oxidant could be injected from the tube or the annulus, and there would be no change in the injection flow area. The use of single-element injectors made performance-limiting effects more readily observable. The performance of both injectors was measured in terms of characteristic-exhaust-velocity efficiency (ratio of experimental to theoretical characteristic exhaust velocity) for various chamber lengths, oxidant-fuel weight ratios, and total propellant flow rates. The performance of these two injectors is compared with that of the vaporization model of reference 3 and the mixing model of reference 4.

APPARATUS AND PROCEDURE

The combustor, composed of injectors, chamber sections, and a nozzle, is illustrated in figure 1. The combustor diameter was 2 inches and the contraction ratio 10; the nominal thrust was 200 pounds. The chamber pressure varied from approximately 150 to 450 pounds per square inch absolute.

Injectors

Two stainless-steel interchangeable injectors were used, each having a single injection element consisting of two coaxial tubes, one for each propellant. The injection pattern is therefore an annular flow of one propellant surrounding tubular flow of the other propellant. The injectors were designed so that the oxidant flow area, whether tubular or annular, was constant, as shown in table I. The hydrogen, however, had a slightly greater flow area when injected from the annulus.

Chambers

The chambers were of uncooled copper and were $1\frac{1}{2}$, $4\frac{1}{2}$, and $9\frac{1}{2}$ inches long. They contained pressure-tap holes 3/4 inch downstream from the injector face.

Nozzle

The nozzle, also of copper, had a 3-inch-long convergent approach section to a 1-inch-long throat and divergent exit. Water coolant passages were located near the throat (fig. 1).

Performance Measurements

Combustor performance was evaluated in terms of characteristic-velocity efficiency. The characteristic exhaust velocity c^* was calculated from measurements of chamber pressure, propellant flow rates, and combustor nozzle throat diameter.

Chamber pressure was measured with a strain-gage-type transducer. It was coupled to the chamber by a short length of small-diameter tubing terminating in a hole located in the chamber wall 3/4 inch downstream from the injector face. The transducer output was recorded on an oscillograph and displayed on a panel meter.

The liquid-oxygen flow rate was measured with a turbine-type flowmeter whose electrical output was a frequency proportional to flow rate. This signal, after being converted to a direct-current voltage was also recorded on an oscillograph and simultaneously displayed on a panel meter.

The gaseous-hydrogen flow was calculated from the upstream pressure and the throat temperature measured by a sonic-orifice flowmeter. These were also recorded on the oscillograph and displayed on panel meters.

The presence of high-frequency or transient combustion pressure phenomena was detected by a water-cooled piezoelectric transducer having a frequency response flat to 10,000 cycles per second. This transducer was mounted flush with the inside surface of the chamber 3/4 inch downstream from the injector face. Its output was also recorded on an oscillograph and on occasion was displayed on an oscilloscope and photographed in order to obtain maximum frequency resolution.

The maximum possible random error in c^* measurements with this instrumentation was approximately $\pm 2\frac{1}{2}$ percent.

Performance Evaluation

The combustor was operated with predetermined total propellant weight flows and oxidant-fuel weight ratios. At least three 2-second runs were used to determine c^* at each flow rate.

The panel meters were locked simultaneously at a predetermined time during the runs, and their retained readings were the primary sources of input for the c^* calculations. The oscillograph records were inspected for any unusual flow or pressure changes not revealed by the panel meters. Runs having any flow perturbations or variations in mean chamber pressure were not used.

Spray Photographs

Liquid-oxygen spray photographs were obtained for both injectors (fig. 2). These show qualitatively the spray characteristics produced by the injectors. Gaseous nitrogen injected at a sonic velocity at the rate of approximately

0.13 pound per second was substituted for gaseous hydrogen. Liquid-oxygen flow rates corresponded to the extremes of operating conditions for this study, 0.2 and 0.4 pound per second.

RESULTS AND DISCUSSION

The averaged experimental data for each series of runs at each flow rate are given in tables II and III. The experimental values of c* efficiency as a function of oxidant-fuel weight ratio o/f are presented in figure 3 for each injector configuration and chamber length.

From figure 3, it may be seen that the effect of oxidant flow rate was small, and had little, if any, effect on combustion efficiency. There is, however, a marked effect of injection configuration on performance. For most conditions, higher performance was obtained when liquid oxygen was annularly injected.

This may be seen more readily in figure 4, where c^* efficiency is presented as a function of chamber length with o/f as a parameter. The curves were prepared by cross plotting the curves faired through the data points in figure 3. Figure 4 shows that, for a given o/f and chamber length, performance is higher when oxygen is annularly injected. The only exception is for very low values of o/f in short chambers.

The performance differences between the two injectors may be partly explained by the photographs of the liquid-oxygen sprays in figure 2. The sprays from annularly injected liquid oxygen are better dispersed and more highly atomized than the tubularly produced sprays.

Further explanation for these results was sought with the vaporization model of reference 3 (eq. (102)), which relates c* efficiency to combustor geometry, chamber pressure, propellant injection temperature, injection velocity, and initial drop size. This model is based on the assumption that performance is limited by the vaporization rate of the less volatile propellant.

All the experimental operation conditions required for the vaporization model are known except the initial liquid-oxygen drop size. This was calculated from equation (102) and figures 24(b) and 29(d) of reference 3 and the appropriate experimental conditions. The results are shown in figure 5. In this figure, the mass median drop size required by the vaporization model to predict the experimental performance is shown as a function of o/f, with chamber length as a parameter for the two injection methods. When the drop sizes were calculated, it was found that a size distribution (geometric standard deviation) of 1.54 best correlated the annular oxygen data, while a distribution of 2.3 was needed for the tubular oxygen data. A spray with a smaller size distribution will have more uniformly sized drops than one with a large distribution.

With annularly injected oxygen, the drop size is completely independent of o/f and only slightly dependent on chamber length. With tubularly injected oxygen, the drop size depends on both the o/f and the chamber length. The model of reference 3 assumes that the initial drop size produced by a given

injector is independent of chamber length.

The ability of this model to correlate data on the basis of initial drop size may, therefore, be used as one criterion of its applicability for a particular situation. The curves of figure 5, therefore, suggest that performance may be vaporization limited, as defined by this model, for annularly injected oxygen but most probably not for tubularly injected oxygen.

Another explanation for the performance of the two injectors may be found by considering the performance to be mixing limited. The intensity of turbulence for both injectors required to predict the experimental performance is presented in figure 6. In this figure, the intensity of turbulence required to predict the experimental performance is shown as a function of chamber length for the two injection methods. The intensities of turbulence were calculated with the model of reference 4. This model relates the mixing efficiency, given in terms of a relative concentration gradient across the chamber, to a mixing parameter $T\left(\frac{x}{s}\right)$, where T is the intensity of turbulence, x the downstream distance from the injector, and s the hole spacing between elements of the injector. If the metered or overall o/f is known, the relative concentration gradient may be transformed to an o/f gradient. The combustor may then be considered to be a composite of many small combustors, each burning at an o/f of a particular region of this gradient. The ratio of the composite c^* for these many small combustors to the theoretical c^* corresponding to the metered o/f is then the efficiency of a combustor whose efficiency is limited by incomplete mixing. For the combustor of this study, it was assumed that the effective injector hole spacing was 2 inches and that the mixing length included the chamber and the 3-inch-long convergent nozzle section.

The results of these calculations (fig. 6) indicate a higher turbulence level for annularly injected oxygen. It is also seen that for both injection methods the turbulence level decreases with chamber length. This decrease in turbulence level with chamber length is in agreement with the results of references 5 and 6.

This analysis indicates that greater turbulence helps to produce higher performance when the least volatile propellant, in this case, liquid oxygen, is injected from the annulus. This would seem to be reasonable, because the propellant injected from the tube, being in this case gaseous, will rapidly expand at the tube exit, tend to fill the combustor volume surrounding the tube, and in so doing create high turbulence and mixing, which will result in higher performance.

It cannot be concluded from these results alone that performance was limited by mixing. But, in view of the results obtained from the vaporization model, it is possible that the performance was limited by poor mixing for tubularly injected oxygen.

The noise level of the combustion was evaluated in terms of the ratio of peak-to-peak values of chamber pressure disturbances to average chamber pressures. The noise, as measured with the high-frequency piezoelectric transducer, usually ranged from approximately 150 to 300 cycles per second but was random within this range. Comparison of the high-frequency sensitive transducer signals with the strain-gage signals indicated that the strain-gage records were a true

indication of both mean and transient chamber pressures.

In figure 7, noise level is presented as a function of o/f for both injectors at each chamber length. The noise level is considerably higher for the tubularly injected oxygen. Except for the case of tubularly injected oxygen in the $1\frac{1}{2}$-inch chamber, the noise level did not depend on the total propellant flow rate. The noise level for tubularly injected oxygen, however, as shown in figure 7(a), increased with decreasing oxygen flow rate. The noise level was always less than 10 percent of mean chamber pressure for annularly injected oxygen, but was as great as 28 percent for tubularly injected oxygen. This indicates that combustion was smoother and more uniform when the less volatile propellant was injected from the annulus.

The high noise level at the low oxygen flow rate with tubularly injected oxygen may perhaps be correlated with the appearance of the sprays shown in figure 2. These photographs show uneven liquid distribution for tubularly injected oxygen at the low flow rate. At the higher flow rate, the spray appears to be more uniform. This uneven liquid distribution at the low flow rate may have been a cause of rough and noisy combustion.

It was also noted that the stainless-steel face of the tubular oxygen injector was discolored because of high temperatures, whereas the other injector showed no discoloration. Preliminary tests were also conducted with a multielement annular oxygen injector whose stainless-steel face was regeneratively cooled with liquid oxygen. These tests also indicated a satisfactorily low heat-transfer rate with the annular oxygen injector. Thus, the problem of cooling the injector face will probably be less severe if the less volatile propellant is injected from the annulus.

CONCLUDING REMARKS

Because of many necessary simplifying assumptions in the turbulent-mixing and vaporization models and the simultaneous occurrence of mixing and vaporization, not to mention many other phenomena, it is difficult to separate the mixing and vaporization effects in this study. Analysis of the data with both models, together with a consideration of the injection process, does, however, permit several conclusions to be drawn.

The vaporization model failed to correlate the data for tubularly injected oxygen. This would suggest either that the performance was limited by some process other than vaporization or that vaporization occurred in a manner not described by the model. Since the oxygen had to diffuse over a relatively long mixing length, that is, the radius of the chamber, it is reasonable to assume that mixing was an important limiting step in the combustion process when oxygen was tubularly injected.

In contrast, the vaporization model correlated the data for annularly injected oxygen fairly well. This by itself would be an insufficient basis on which to conclude that the performance was vaporization limited. It would be assumed that the mixing in this case was relatively rapid, because of the expansion of the hydrogen into the oxygen stream, and was, therefore, not a

controlling factor in the combustion process. It is, therefore, reasonable to conclude that the performance was vaporization limited.

It may also be pointed out that other changes in a combustor may determine the rate-limiting process. For example, in reference 7, a change in contraction ratio, with no other design changes, appeared to shift combustor performance from a vaporization-limited region to a mixing-limited region. Thus, these models must be carefully applied, but they are useful in understanding the combustion process and in designing new combustors.

SUMMARY OF RESULTS

Performance, evaluated in terms of characteristic-velocity efficiency, was determined for a gaseous-hydrogen - liquid-oxygen combustor with coaxial propellant injection. The purpose of the study was to compare performance with the less volatile propellant injected from the tube and from the annulus. The combustor nominal thrust was 200 pounds; the chamber diameter was 2 inches and the contraction ratio 10. The chamber pressure varied from approximately 150 to 450 pounds per square inch absolute. The chamber length was varied from $1\frac{1}{2}$ to $9\frac{1}{2}$ inches, and the nozzle length was 3 inches. The oxidant-fuel weight ratio was varied from approximately 1.5 to 10. The weight flow of oxygen was varied from 0.2 to 0.4 pound per second over the entire o/f range of oxidant-fuel ratio. The following results were obtained:

1. With coaxial injection and all operating conditions equal, performance was higher when the less volatile propellant, liquid oxygen, was injected from an annular area surrounding the more volatile propellant, gaseous hydrogen, than when the oxygen was injected from a central tube.

2. Analysis of the data in accordance with a vaporization-limited analytical model did not completely correlate the results for tubularly injected liquid oxygen but did correlate the data for annularly injected liquid oxygen. The analysis indicated smaller, more uniformly sized drops for annularly injected oxygen.

3. The level of turbulence required by a mixing model to predict the experimental performance indicated that turbulence levels were higher when liquid oxygen was injected from the annulus. This suggested that the performance may have been mixing limited when the oxygen was tubularly injected.

4. Combustion noise was lower when liquid oxygen was annularly injected and was independent of oxidant-fuel ratio. When the oxygen was tubularly injected, the combustion noise was considerably higher at low oxidant-fuel ratios and tended to increase with decreasing oxygen flow rate.

5. Heat transfer to the injector face, as indicated by discoloration of the face, appeared to be higher when the oxygen was tubularly injected.

Lewis Research Center
National Aeronautics and Space Administration
Cleveland, Ohio, November 4, 1963.

REFERENCES

1. Stein, Samuel: A High-Performance 250-Pound-Thrust Rocket Engine Utilizing Coaxial-Flow Injection of JP-4 Fuel and Liquid Oxygen. NASA TN D-126, 1959.

2. Heidmann, M. F., and Baker, Louis, Jr.: Combustor Performance with Various Hydrogen-Oxygen Injection Methods in a 200-Pound-Thrust Rocket Engine. NACA RM E58E21, 1958.

3. Priem, Richard J., and Heidmann, Marcus F.: Propellant Vaporization as a Design Criterion for Rocket-Engine Combustion Chambers. NASA TR R-67, 1960. (Supersedes NACA TN's 3883, 3985, 4098, and 4219.)

4. Bittker, David A.: An Analytical Study of Turbulent and Molecular Mixing in Rocket Combustion. NACA TN 4321, 1958.

5. Hersch, Martin: An Experimental Method of Measuring Intensity of Turbulence in a Rocket Chamber. ARS Jour., vol. 31, no. 1, Jan. 1961, pp. 39-46.

6. Ribner, H. S., and Tucker, M.: Spectrum of Turbulence in a Contracting Stream. NACA Rep. 1113, 1953. (Supersedes NACA TN 2606.)

7. Hersch, Martin: Combined Effect of Contraction Ratio and Chamber Pressure on the Performance of a Gaseous-Hydrogen - Liquid-Oxygen Combustor for a Given Propellant Weight Flow and Oxidant-Fuel Ratio. NASA TN D-129, 1961.

TABLE I. - INJECTOR DIMENSIONS

Oxidant injection	Tube inside diameter, in.	Annulus diameter, in.		Oxidant injector area, sq in.	Fuel injector area, sq in.
		Inside	Outside		
Tubular	0.118	0.156	0.335	0.0110	0.0684
Annular	0.251	0.313	0.335	0.0110	0.0491

TABLE II. - EXPERIMENTAL COMBUSTOR DATA FOR TUBULAR OXYGEN INJECTION

(a) Chamber length, $1\frac{1}{2}$ inches

Chamber pressure, lb/sq in. abs	Oxidant flow, lb/sec	Fuel flow, lb/sec	Total flow, lb/sec	Oxidant-fuel weight ratio, o/f	Characteristic exhaust velocity, c*	
					Experimental, ft/sec	Percent of theoretical
307	0.204	0.133	0.337	1.54	7990	97.7
276	.209	.101	.310	2.08	7760	93.8
222	.199	.0689	.268	2.89	7230	87.5
195	.202	.0521	.254	3.88	6700	82.0
169	.199	.0427	.242	4.65	6090	76.4
150	.198	.0352	.233	5.61	5660	71.5
132	.192	.0311	.223	6.18	5160	68.4
335	.315	.0991	.414	3.18	7060	85.4
285	.312	.0760	.388	4.11	6410	78.8
258	.312	.0645	.377	4.84	5950	75.3
225	.312	.0518	.364	6.01	5390	70.9
204	.312	.0453	.357	6.90	5100	69.5
174	.307	.0378	.345	8.11	4580	65.6
437	.393	.130	.523	3.02	7300	87.6
380	.401	.0985	.500	4.07	6650	82.6
333	.401	.0774	.478	5.18	6000	76.5
303	.401	.0661	.467	6.06	5670	74.9
277	.406	.0581	.464	7.00	5200	71.0
258	.406	.0504	.456	8.06	4970	70.7
(b) Chamber length, $4\frac{1}{2}$ inches						
258	0.194	0.0970	0.291	2.00	7830	94.7
230	.210	.0670	.277	3.14	7510	90.6
200	.213	.0523	.265	4.07	6820	83.9
168	.208	.0416	.250	5.01	6060	76.7
150	.208	.0340	.242	6.12	5590	73.8
132	.198	.0286	.227	6.91	5230	71.2
272	.190	.129	.319	1.47	7670	94.5
315	.295	.0978	.393	3.02	7170	86.5
339	.311	.0991	.410	3.14	7440	89.9
286	.312	.0742	.386	4.21	7430	81.6
259	.307	.0641	.371	4.79	6200	77.9
231	.312	.0505	.363	6.19	5690	75.5
210	.300	.0447	.345	6.73	5420	73.4
189	.310	.0374	.347	8.29	4850	69.8
437	.395	.104	.499	3.82	7340	89.7
379	.382	.100	.482	3.82	7070	86.4
339	.403	.0787	.482	5.13	6240	79.4
307	.405	.0665	.472	6.09	5680	75.0
283	.405	.0584	.463	6.94	5450	74.4
267	.405	.0529	.458	7.66	5200	72.9
(c) Chamber length, $9\frac{1}{2}$ inches						
338	0.322	0.0955	0.418	3.37	7700	93.2
284	.302	.0738	.376	4.10	7150	87.9
258	.302	.0616	.364	4.90	6720	84.9
227	.308	.0487	.357	6.33	5980	79.7
209	.308	.0430	.351	7.16	7690	77.0
193	.308	.0370	.345	8.33	5350	76.9
281	.197	.131	.328	1.51	7890	97.0
249	.192	.0990	.291	1.94	7760	94.0
238	.208	.0675	.286	3.08	7790	94.0
221	.204	.0680	.272	3.00	8090	97.5
240	.191	.0985	.290	1.94	8260	100
269	.208	.129	.337	1.61	7970	97.5
199	.212	.0508	.263	4.16	7590	93.5
176	.213	.0417	.255	5.11	6950	88.3
157	.208	.0347	.243	6.00	6480	85.3
136	.198	.0282	.226	7.03	6020	82.3
323	.314	.0964	.410	3.26	7740	93.6
281	.314	.0739	.388	4.25	7100	87.6
213	.312	.0438	.356	7.12	5890	80.9
248	.312	.0621	.374	5.02	6520	82.5
231	.312	.0501	.362	6.23	6300	83.6
195	.307	.0369	.344	8.34	5580	80.3
420	.392	.128	.520	3.07	7930	95.6
375	.395	.0989	.494	4.00	7440	91.8
332	.395	.0785	.474	5.03	6900	87.3
303	.398	.0661	.464	6.02	6410	84.4
285	.400	.0754	.475	6.98	6160	84.2
267	.400	.0513	.451	7.80	5840	82.3

TABLE III. - EXPERIMENTAL COMBUSTOR DATA FOR ANNULAR OXYGEN INJECTION

(a) Chamber length, $1\frac{1}{2}$ inches

Chamber pressure, lb/sq in. abs	Oxidant flow, lb/sec	Fuel flow, lb/sec	Total flow, lb/sec	Oxidant-fuel weight ratio, o/f	Characteristic exhaust velocity, c^*	
					Experimental, ft/sec	Percent of theoretical
287	0.209	0.132	0.341	1.58	7470	91.6
257	.214	.101	.315	2.12	7290	87.9
213	.198	.0700	.268	2.83	7070	85.1
185	.198	.0519	.250	3.82	6540	80.6
168	.198	.0422	.240	4.69	6110	76.6
159	.201	.0351	.236	5.73	6020	78.3
148	.203	.0293	.232	6.93	5150	77.2
318	.314	.0991	.413	3.17	6870	83.0
272	.317	.0760	.393	4.17	6150	75.9
249	.312	.0642	.376	4.86	5920	74.6
237	.312	.0518	.364	6.03	5820	76.7
228	.312	.0448	.357	6.96	5760	78.6
422	.389	.132	.521	2.95	7200	86.8
385	.395	.101	.496	3.92	6900	84.5
353	.400	.0808	.481	4.95	6460	81.6
328	.400	.0684	.468	5.85	5390	80.6
295	.400	.0584	.458	6.85	5650	76.9

(b) Chamber length, $4\frac{1}{2}$ inches

282	0.210	0.131	0.341	1.61	7980	97.8
256	.203	.0985	.302	2.06	8190	98.9
221	.205	.0664	.271	3.09	7790	94.0
190	.198	.0420	.240	4.71	6730	84.3
174	.206	.0415	.248	4.96	6840	86.5
165	.206	.0347	.241	5.94	6710	87.6
148	.211	.0277	.239	7.64	5900	82.7
344	.322	.0984	.420	3.27	6740	93.0
291	.319	.0812	.400	3.93	6980	85.5
272	.318	.0625	.381	5.09	6660	84.6
245	.322	.0505	.373	6.38	6160	82.3
230	.313	.0433	.356	7.23	6020	83.0
207	.314	.0345	.349	9.10	5540	81.9
456	.392	.128	.520	3.06	8220	99.1
397	.400	.0993	.499	4.03	7420	91.2
375	.394	.0814	.475	4.85	7430	93.6
329	.384	.0665	.451	5.77	6790	88.6
306	.383	.0572	.440	6.70	6500	87.8

(c) Chamber length, $9\frac{1}{2}$ inches

287	0.188	0.129	0.317	1.45	8200	101
274	.200	.0975	.298	2.05	8350	101
256	.209	.0645	.274	3.24	8340	101
232	.208	.0484	.256	4.30	8150	101
211	.206	.0396	.246	5.20	7760	98.9
189	.208	.0314	.239	6.62	7170	96.6
158	.209	.0243	.233	8.61	6150	89.3
220	.211	.0496	.261	4.26	7950	98.2
250	.209	.0668	.276	3.13	8090	97.6
269	.202	.0971	.299	2.08	8210	99.1
287	.202	.125	.327	1.61	7910	96.9
348	.285	.0956	.381	2.98	8180	98.6
327	.279	.0721	.351	3.87	8250	101
316	.295	.0616	.357	4.78	8150	100
279	.303	.0467	.350	6.48	7210	96.6
281	.302	.0477	.350	6.33	7270	96.7
257	.307	.0391	.346	7.85	6810	96.2
223	.300	.0278	.328	10.8	6120	95.4
408	.375	.128	.503	2.94	8000	96.4
387	.370	.0986	.469	3.75	8130	99.2
362	.370	.0779	.448	4.75	7970	100
341	.370	.0659	.436	5.61	7720	100
322	.372	.0551	.427	6.75	4290	101
141	.152	.0282	.180	5.40	7330	94.2
165	.214	.0254	.239	8.42	6140	88.6
161	.202	.0262	.228	7.70	6490	91.2

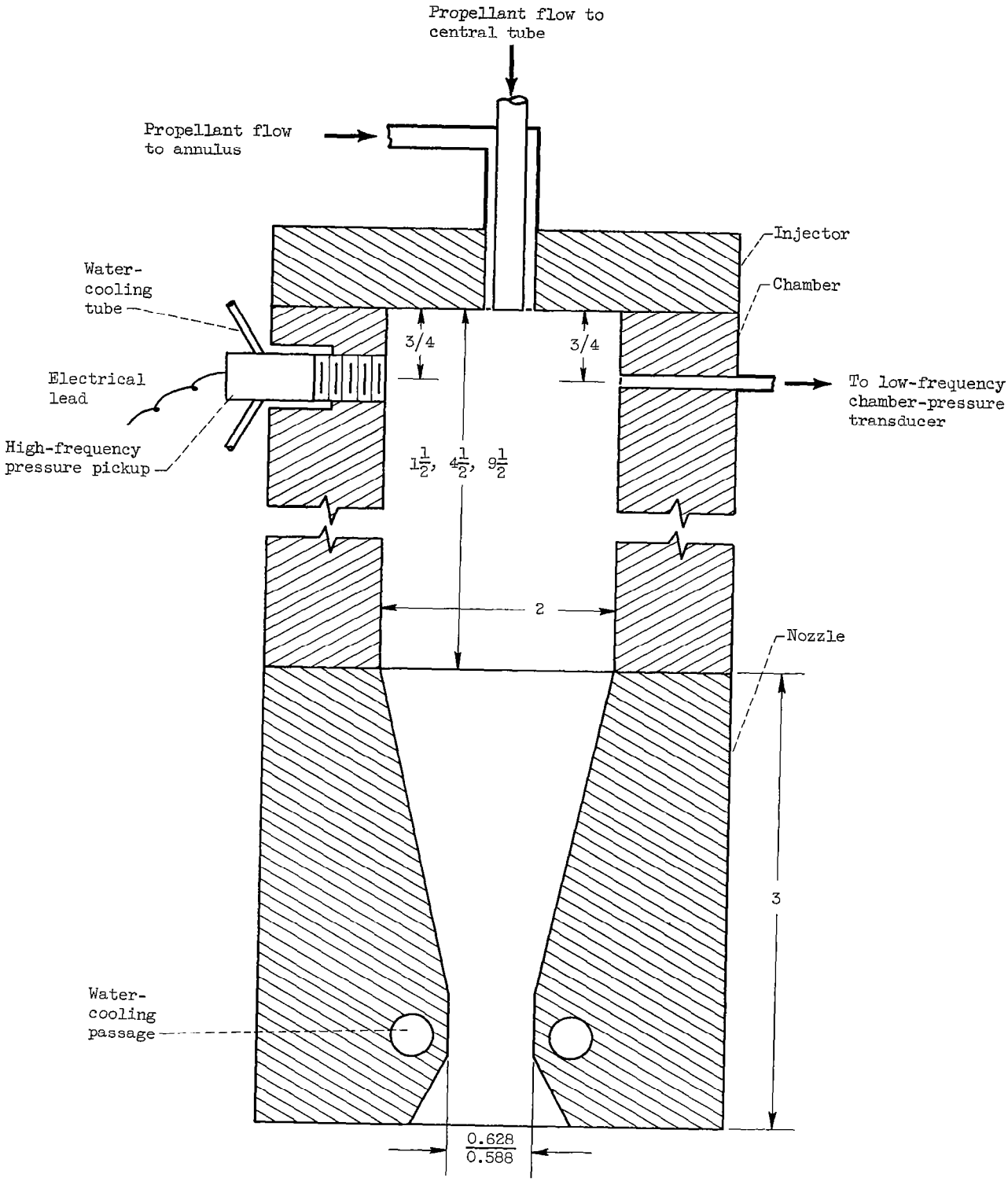

Figure 1. - Schematic drawing of combustor. (Dimensions in inches.)

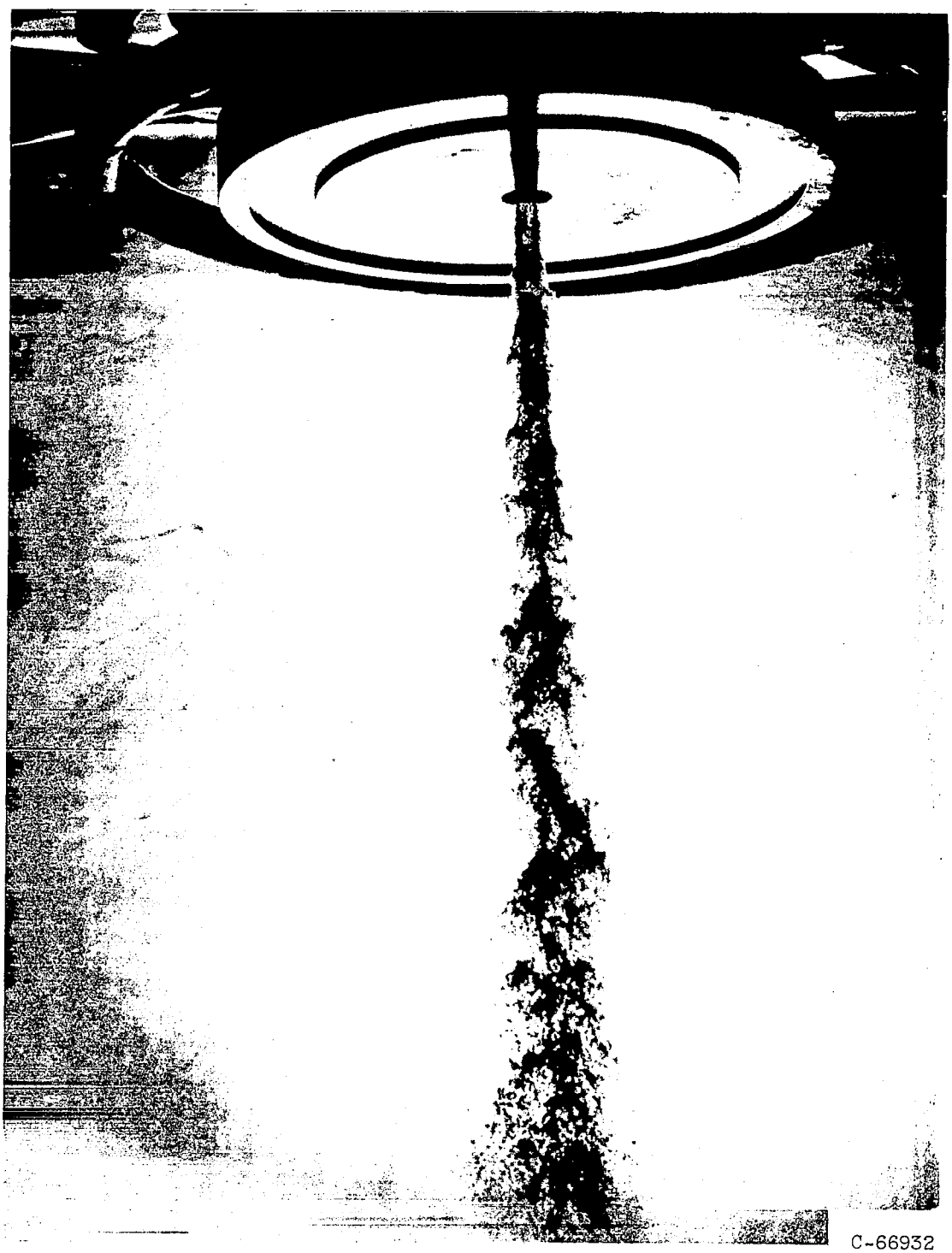

(a) Oxygen in tube. Oxygen flow, 0.2 pound per second.

Figure 2. - Liquid-oxygen - gaseous-nitrogen spray. Sonic nitrogen flow, approximately 0.13 pound per second.

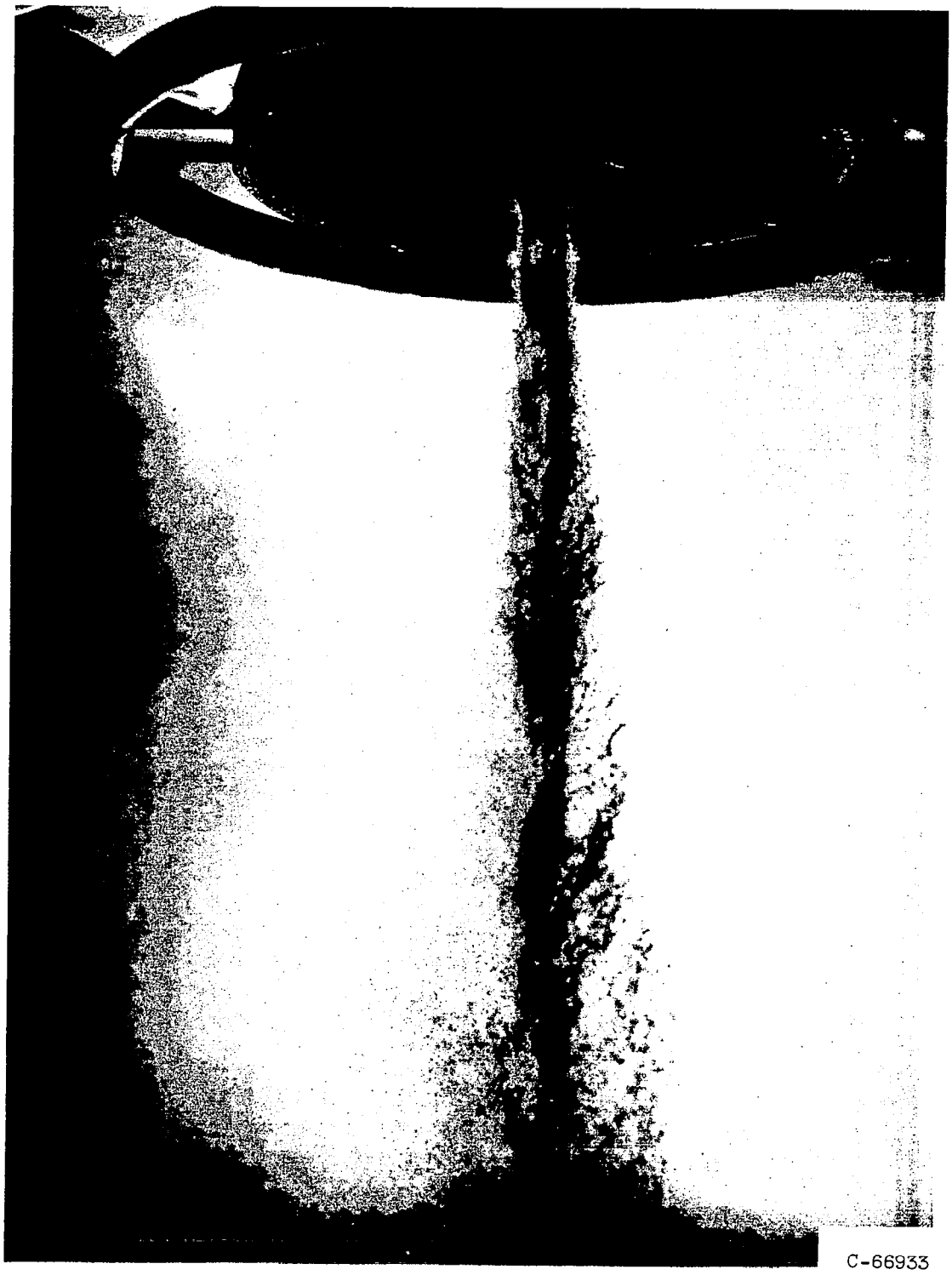

(b) Oxygen in annulus. Oxygen flow, 0.2 pound per second.

Figure 2. - Continued. Liquid-oxygen - gaseous-nitrogen spray. Sonic nitrogen flow, approximately 0.13 pound per second.

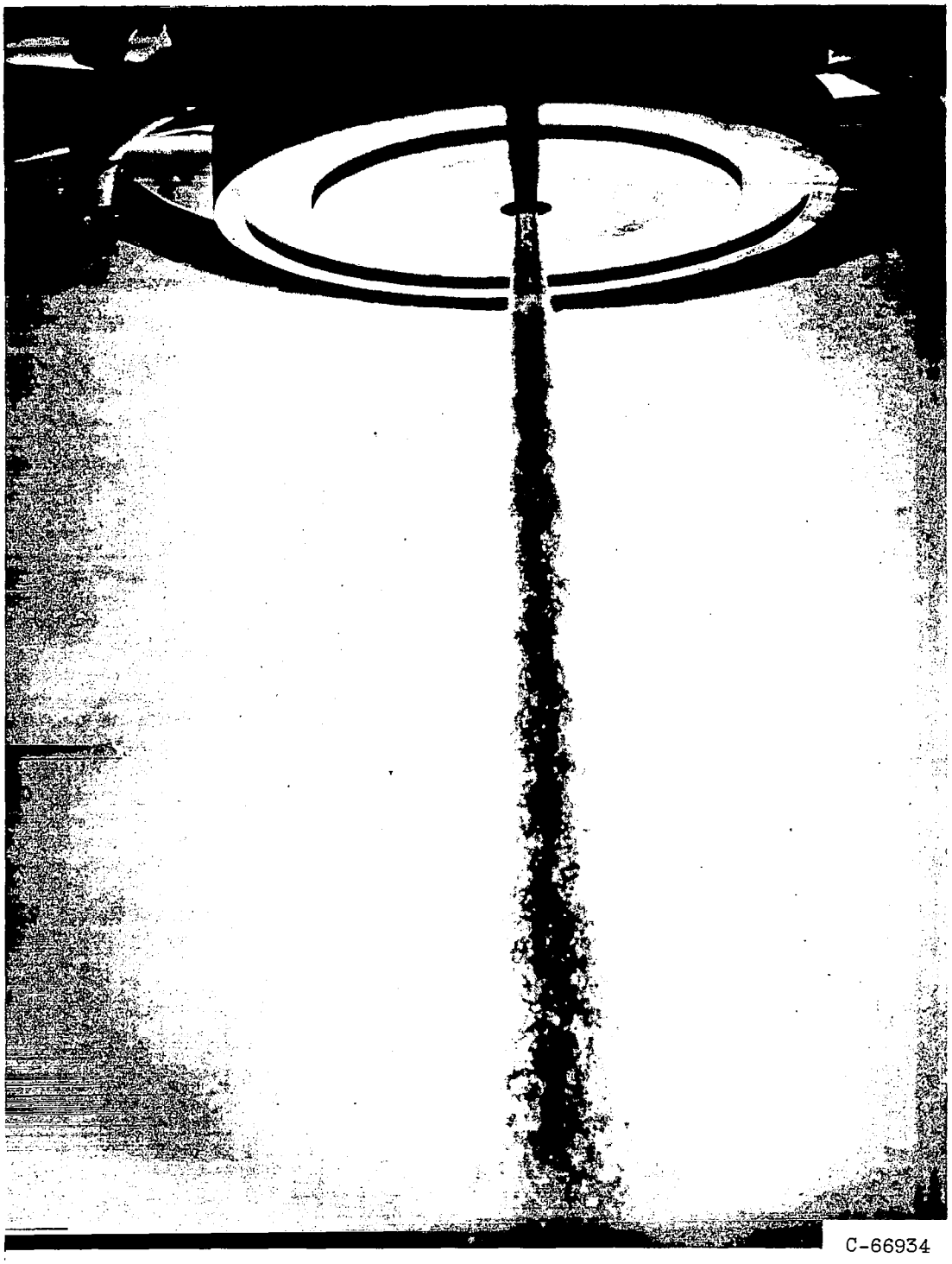

(c) Oxygen in tube. Oxygen flow, 0.4 pound per second.

Figure 2. - Continued. Liquid-oxygen - gaseous-nitrogen spray. Sonic nitrogen flow, approximately 0.13 pound per second.

(d) Oxygen in annulus. Oxygen flow, 0.4 pound per second.

Figure 2. - Concluded. Liquid-oxygen - gaseous-nitrogen spray. Sonic nitrogen flow, approximately 0.13 pound per second.

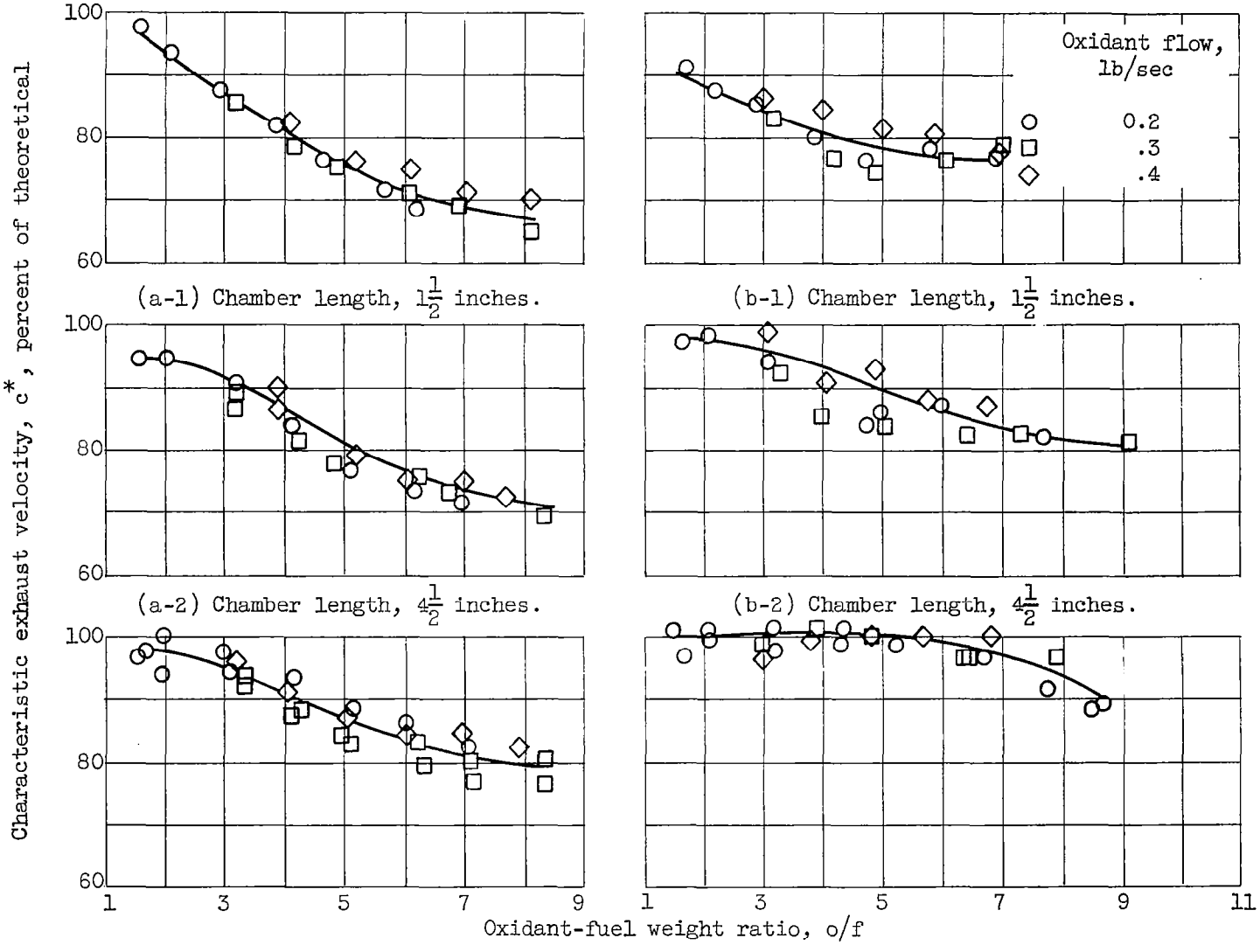

(a) Tubular oxygen injection.

(b) Annular oxygen injection.

Figure 3. - Variation of combustor performance with oxidant-fuel weight ratio.

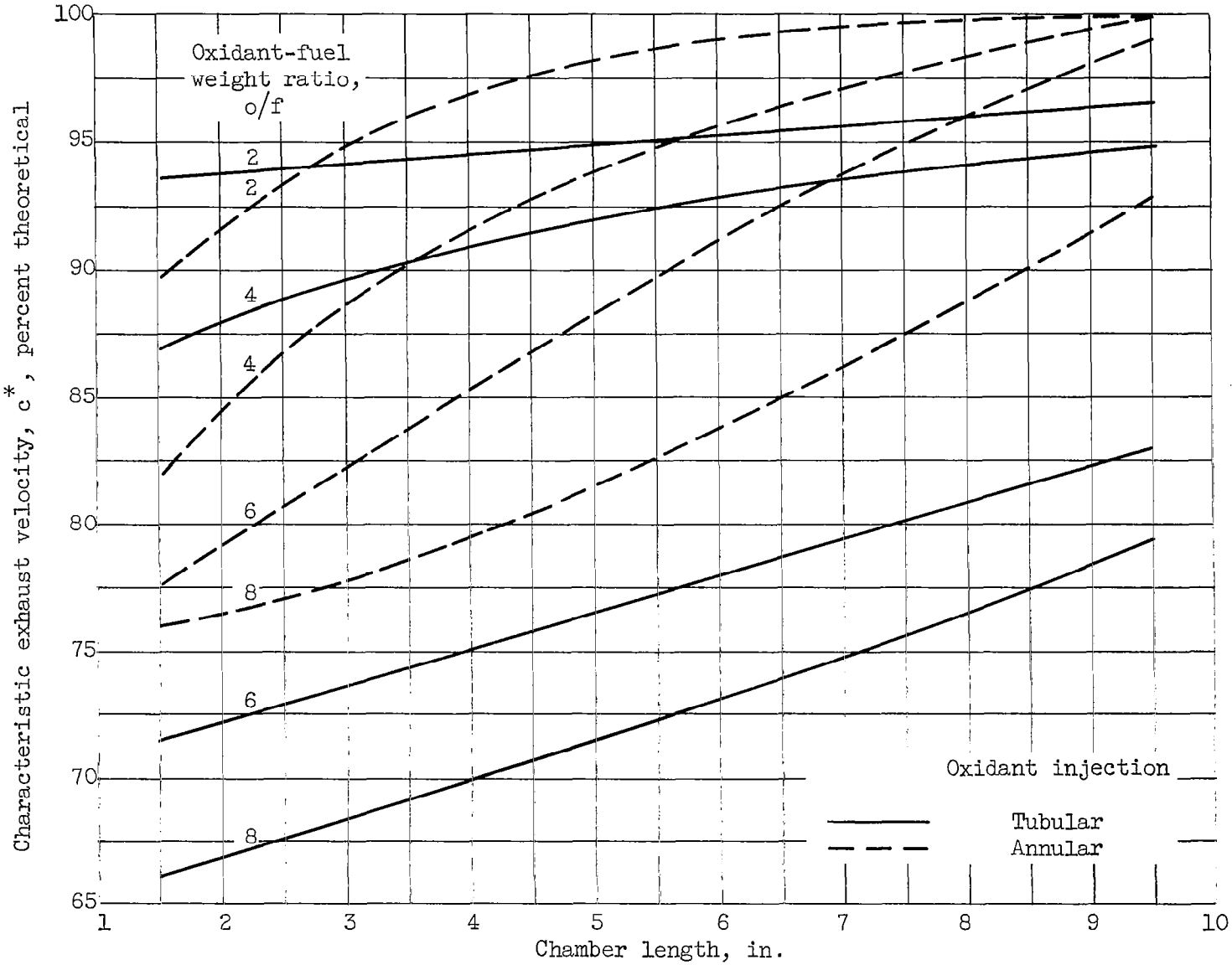

Figure 4. - Variation of combustor performance with chamber length.

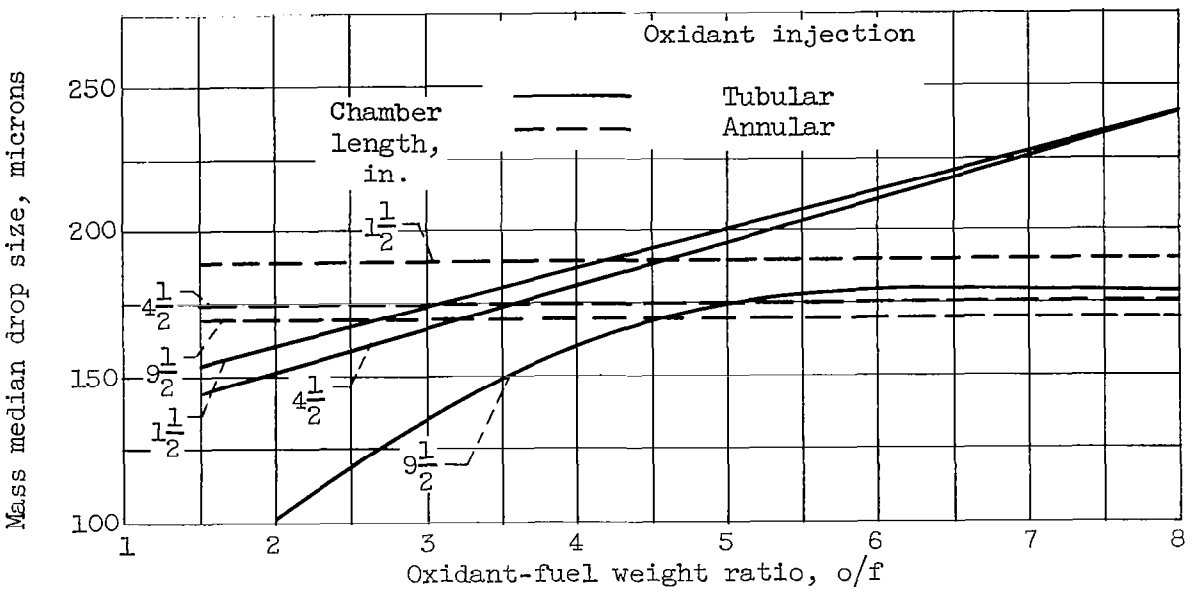

Figure 5. - Averaged data showing effect of chamber length and oxidant-fuel weight ratio on mass median drop size.

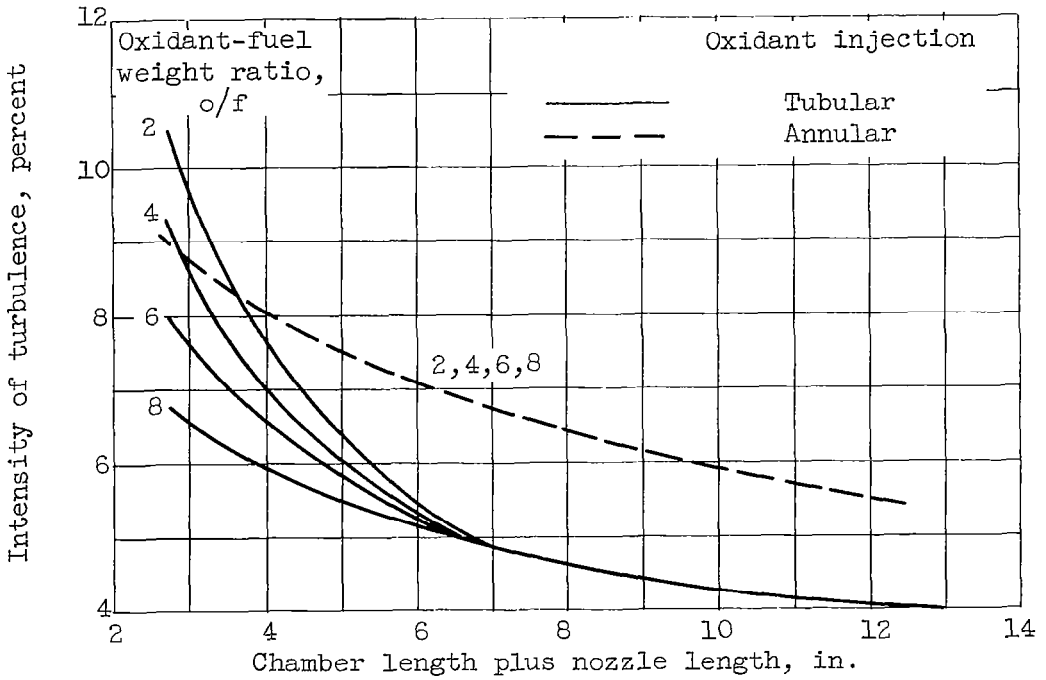

Figure 6. - Averaged data showing effect of chamber length on intensity of turbulence with oxidant-fuel weight ratio as a parameter.

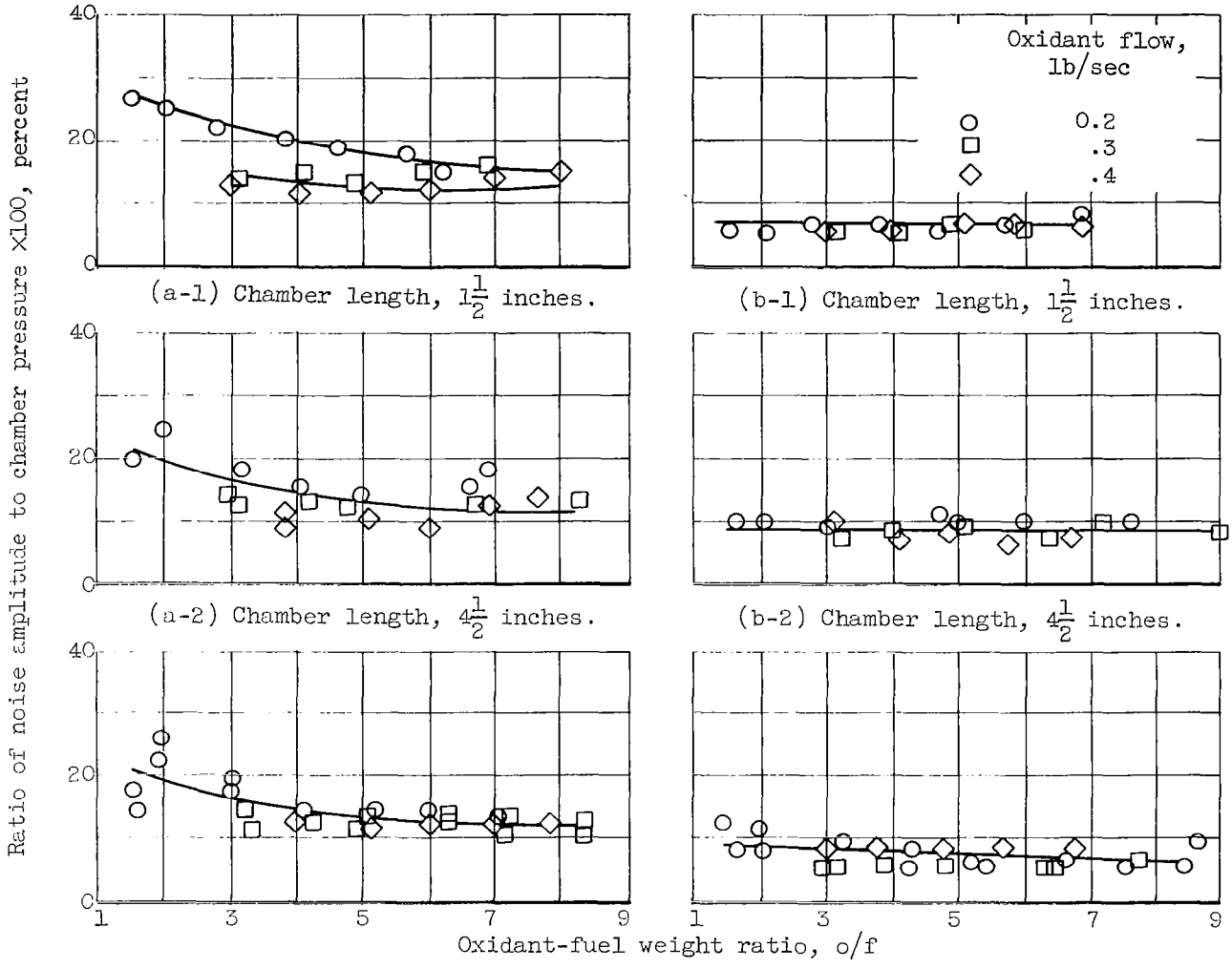

(a) Tubular oxygen injection.

(b) Annular oxygen injection.

Figure 7. - Variation of combustion noise with oxidant-fuel weight ratio.